

Fast and Slow Gating of CLC-1: Differential Effects of 2-(4-Chlorophenoxy) Propionic Acid and Dominant Negative Mutations

E. C. AROMATARIS, G. Y. RYCHKOV, B. BENNETTS, B. P. HUGHES, A. H. BRETAG, and M. L. ROBERTS

Department of Physiology, University of Adelaide, Adelaide, South Australia, Australia (E.C.A., G.Y.R., B.B., A.H.B., M.L.R.); and Centre for Advanced Biomedical Studies, University of South Australia, Adelaide, South Australia, Australia (G.Y.R., B.P.H., A.H.B.)

Received December 14, 2000; accepted April 5, 2001

This paper is available online at <http://molpharm.aspetjournals.org>

ABSTRACT

Our knowledge about CLC-1 muscle chloride channel gating, previously gained from single-channel recording and noise analysis, provides a theoretical basis for further analysis of macroscopic currents. In the present study, we propose a simple method of calculation of open probabilities (P_o) of fast and slow gates from the relative amplitudes of CLC-1 inward current components. With this method, we investigated the effects of 2-(4-chlorophenoxy) propionic acid (CPP), a drug known to produce myotonia in animals, and dominant negative myotonic mutations, F307S and A313T, on fast and slow gating

of CLC-1. We have shown that these mutations affected the P_o of the slow gate, as expected from their mode of inheritance, and that CPP predominantly affected the fast gating process. CPP's action on the fast gating of mutant channels was similar to its effect in wild-type channels. Comparison of the effects of CPP and the mutations on fast and slow gating with the effects produced by reduction of external Cl^- concentration suggested that CPP and mutations exert their action by affecting the transition of the channel from its closed to open state after Cl^- binding to the gating site.

Many physiologically important functions, including regulation of cell volume, transepithelial transport, and electrical excitability rely on members of the large CLC family of voltage-dependent chloride channels (for review, see Jentsch et al., 1999). Mutations in three of these result in human hereditary disorders, including myotonia, Bartter's syndrome, and Dent's disease (Koch et al., 1992; Lloyd et al., 1996; Simon et al., 1997). The skeletal muscle disease myotonia congenita is associated with mutations in *CLCN1*, the gene encoding the major skeletal muscle chloride channel, CLC-1, and can be inherited in two forms, the autosomal recessive Becker's disease or the autosomal dominant Thomsen's disease (Koch et al., 1992). Almost all mutations resulting in Thomsen's disease exert a dominant negative effect on CLC-1 function and result in a shift in the voltage dependence of CLC-1 gating to more positive potentials (Pusch et al., 1995b; Wollnik et al., 1997; Kubisch et al., 1998). This shift in the voltage dependence of gating accounts for the reduced chloride conductance (G_{Cl}) seen in myotonic muscle fibers.

Langer and Levy (1968) reported that clofibrate, once commonly used to treat hyperlipidemia, induced a syndrome

characterized by muscle stiffness and weakness. In experimental animals, it has been possible to simulate myotonic symptoms, similar to those produced by mutations in CLC-1, using treatment with clofibrate and its analogs (Bryant and Morales-Aguilera, 1971; Dromgoole et al., 1975; Conte Camerino et al., 1988). Two recent studies investigating the effects of 2-(4-chlorophenoxy) propionic acid (CPP), the most potent of the clofibrate analogs, on the wild-type (WT) CLC-1 channel showed that this drug causes changes in CLC-1 properties similar to those found in the myotonic mutant channels: it shifts the voltage dependence of activation of the CLC-1 channel to more positive potentials (Aromataris et al., 1999; Pusch et al., 2000). Because CLC-1 gating depends on Cl^- binding in the channel pore and P_o of CLC-1 shifts when the external Cl^- concentration is changed (Rychkov et al., 1996), it was hypothesized that CPP reduces the affinity of the gating site of CLC-1 for Cl^- (Aromataris et al., 1999). The apparent similarity of action between drug and naturally occurring mutations may indicate that the binding of CPP to its specific binding site produces a change in the channel protein similar to those produced by dominant missense mutations in CLC-1.

The fact that chemical agents can interact with the gating process of CLC-1 suggests that it may be possible to develop a drug that would shift the gating of mutant versions of CLC-1

This work was supported by the Neuromuscular Research Foundation of the Muscular Dystrophy Association of South Australia and the Australian Research Council.

ABBREVIATIONS: CPP, 2-(4-chlorophenoxy) propionic acid; WT, wild-type; P_o , open probability; PCR, polymerase chain reaction; HEK, human embryonic kidney.

back toward more negative potentials; therefore, closer scrutiny of the mechanisms of gating are warranted. Recent advances in the area (Saviane et al., 1999; Accardi and Pusch, 2000), and a method for the separation of the P_o of fast and slow gating from the whole-cell currents proposed in the present article has allowed us to investigate further the properties of mutant channels and to compare them with the changes introduced by application of CPP. The results indicate that the F307S and A313T mutations shift P_o of slow gating, as expected from their dominant mode of inheritance, without significant effect on fast gating. CPP, by contrast, mainly affects fast gating in the WT and mutant channels.

Materials and Methods

Site-Directed Mutagenesis. Point mutations were introduced into hCIC-1 cDNA (Steinmeyer et al., 1994) by standard two-step PCR-based site-directed mutagenesis (Ho et al., 1989). PCRs were performed using *Pwo* DNA polymerase (Roche Molecular Biochemicals, Mannheim, Germany) for high fidelity amplifications. Two fragments were amplified in the first step, using primers containing the desired mutation in a short overlapping region and pTLN-hCIC-1 (Lorenz et al., 1996) as a template. In the second step, the two partial overlapping fragments were joined by recombinant PCR. The final products were digested with the appropriate restriction endonucleases and ligated into the pTLN-hCIC-1 vector. Restriction endonucleases were used to isolate appropriate fragments carrying the desired mutation in hCIC-1, which were then ligated into the pCIneo (Promega, Madison, WI) mammalian expression vector. All PCR-derived fragments were entirely sequenced to exclude any polymerase errors.

Cell Culture and Transfection. Human embryonic kidney (HEK293) cells were grown in Dulbecco's modified Eagle's medium (Invitrogen Australia, Melbourne, Australia) containing 10% (v/v) fetal bovine serum (Trace, Melbourne, Australia), supplemented with L-glutamine (20 mM; Sigma, St. Louis, MO) and maintained at 37°C with 5% CO₂. Twenty-four hours after cell cultures were split, cells were transfected with 0.8 μg of either WT or mutant pCIneo-hCIC-1 cDNA using LipofectAMINE PLUS reagent (Invitrogen), following the standard protocol described by the manufacturer, in 25-mm culture wells. To allow ready identification of transfected cells during patch-clamp experiments, cells were cotransfected with ~0.1 μg of green fluorescent protein plasmid cDNA (pEGFP-N1; CLONTECH, Palo Alto, CA). Approximately 6 h after transfection, cells were replated ready for patch clamping. Electrophysiological measurements were commenced 25 h after transfection.

Electrophysiology. Patch-clamp experiments on HEK293 cells were performed in the whole-cell configuration at room temperature (24 ± 1°C) using a List EPC 7 (List, Darmstadt, Germany) patch-clamp amplifier and associated standard equipment. The standard bath solution contained 170 mM NaCl, 2 mM MgCl₂, 2 mM CaCl₂, 10 mM HEPES, adjusted to pH 7.4 with NaOH. The standard pipette solution contained 40 mM CsCl, 110 mM Cs-glutamate, 10 mM EGTA-K, 10 mM HEPES, adjusted to pH 7.2 with NaOH. Lower external Cl⁻ concentrations were achieved by equimolar substitution of Na-glutamate for NaCl, whereas the high external Cl⁻ concentration (i.e., 356 mM Cl⁻) was achieved by doubling the concentrations of all solutes present, except HEPES in the bath solution and HEPES and EGTA-K in the pipette solution. All data presented in the figures were obtained at 178 mM Cl⁻ in the external solution, except were specified.

Patch pipettes of 1 to 4 MΩ were pulled from borosilicate glass and coated with Sylgard (Dow Corning, Midland, MI). Series resistance did not exceed 5 MΩ and was 75 to 85% compensated. Currents obtained were filtered at 3 kHz, collected, and analyzed using pCLAMP software (Axon Instruments, Foster City, CA). Potentials listed are pipette potentials expressed as intracellular potentials relative to outside zero. Liquid junction potentials between the bath

and electrode solutions were estimated with the use of JPCalc (Barry, 1994) and corrected for in all data presented on graphs and in Table 1.

Chemicals. (R,S)-(±)-CPP was obtained from Sigma. The sodium salt of this compound, which was prepared by neutralizing the corresponding acid with an equimolar amount of NaOH (added as a 1 M solution), was dissolved in freshly made bath solution as required.

Data Analysis. Single channel recording of CIC-1 recently performed by Saviane et al. (1999) is consistent with the presence of two independent gates in this channel: a fast gate that works on each single protopore and a slow gate that gates both protopores simultaneously. Time constants of the fast and slow gates obtained from single-channel recordings are very similar to the time constants of two exponential components that can be fitted to the macroscopic currents. Accepting that the time constants extracted from whole cell currents reflect relaxations of the fast and slow gates, it is possible to derive the open probabilities of fast and slow gates from the relative amplitudes of the corresponding exponential components. During the voltage step from a membrane potential of V_1 to the membrane potential V , the P_o of each gate changes exponentially from one steady state to another. Dependence of the P_o of the fast gate on time can be described by the following equation:

$$P_V^f(t) = (P_{V_1}^f - P_V^f) \cdot e^{-t/\tau_f} + P_V^f \quad (1)$$

where $P_{V_1}^f$ and P_V^f are the steady state P_o of the fast gate at the membrane potential V_1 and V , respectively, and τ_f is the time constant of the fast gate.

Similarly, for the slow gate:

$$P_V^s(t) = (P_{V_1}^s - P_V^s) \cdot e^{-t/\tau_s} + P_V^s \quad (2)$$

where τ_s is the time constant of the slow gate.

The open probability of the channel overall is given by the equation:

$$P_V(t) = P_V^f(t) \cdot P_V^s(t) \quad (3)$$

If the initial voltage V_1 is set positive to +40 mV, P_o of the fast and slow gates is near unity (Saviane et al., 1999). Consequently, the result of multiplication of open probabilities of the fast and slow gates will be as follows:

$$P_V(t) = (1 - P_V^f)P_V^s e^{-t/\tau_f} + (1 - P_V^s)P_V^f e^{-t/\tau_s} + (1 - P_V^f) \cdot (1 - P_V^s) e^{-t \left(\frac{\tau_s + \tau_f}{\tau_s \tau_f} \right)} + P_V^f P_V^s \quad (4)$$

This equation contains three exponential terms; however, it can be simplified making the following assumption: $e^{-t \left(\frac{\tau_s + \tau_f}{\tau_s \tau_f} \right)} \approx e^{-t/\tau_f}$ when τ_s is much greater than τ_f . In CIC-1, the time constant of slow gating τ_s is 3 to 10 times slower than time constant of fast gating τ_f depending on the experimental conditions (Fahlke et al., 1996; Rychkov et al., 1996; Saviane et al., 1999; Accardi and Pusch, 2000). The smallest difference between τ_f and τ_s in the present work was obtained for A313T mutant at -120 mV: 5 ms and 13 ms, respectively. The time constant of the third exponential component in eq. 4 in this case would be 3.6 ms. Under the present experimental conditions, exponential components with time constants of 3.6 ms and 5 ms are indistinguishable, so the above assumption is valid for all experimental conditions in the present study. Consequently, time dependence of the P_o of the channel can be described by the following equation:

$$P_V(t) = (1 - P_V^f) \cdot e^{-t/\tau_f} + (1 - P_V^s)P_V^f \cdot e^{-t/\tau_s} + P_V^f P_V^s \quad (5)$$

The time dependence of the current relaxation is given by the equation:

$$I_V(t) = I_{\max} \cdot P_V(t) \quad (6)$$

where I_{\max} is the peak current at time 0.

On the other hand, the raw current data points can be fitted with an equation comprising two exponential components:

$$I_V(t) = A_1 e^{-t/\tau_1} + A_2 e^{-t/\tau_2} + C \quad (7)$$

where A_1 , A_2 , and C are the amplitudes of the fast, slow, and steady-state components of the current, respectively. Combining eqs. 5, 6, and 7 and dividing it by I_{\max} , it is possible to show that the solution of the final equation at each time point exists only if $\tau_f = \tau_1$; $\tau_s = \tau_2$ and the coefficients in front of the corresponding exponentials are equal. Consequently,

$$P_V^f = 1 - a_1 \quad (8)$$

and

$$P_V^s = \frac{c}{a_2 + c} \quad (9)$$

where a_1 , a_2 , and c are A_1/I_{\max} , A_2/I_{\max} , and C/I_{\max} , respectively.

Normalized peak tail currents for voltage steps to -100 mV for WT and -60 mV for mutants after test pulses in the range from -160 to $+120$ mV were used to produce apparent P_o curves by fitting with a Boltzmann distribution with an offset, of the form:

$$P_o(V) = P^{\min} + \frac{1 - P^{\min}}{1 + \exp((V_{1/2} - V)/k)} \quad (10)$$

where P^{\min} is an offset, or a minimal P_o at very negative potentials, V is the membrane potential, $V_{1/2}$ is the half-maximal activation potential, and k is the slope factor. A Boltzmann distribution of this form presumes that the maximal P_o is always 1. The same equation was used to produce P_o curves for the fast and slow gates with the data points calculated by using eqs. 8 and 9.

There are some limitations to the method of separation of P_o of the fast and slow gates that should be considered. The assumption that maximal P_o reaches unity at potentials positive to $+40$ mV seems to be true for WT channel in the control conditions (Saviane et al., 1999); however, this is not necessarily true for mutant channels or for WT channels in the presence of some blockers or foreign anions. This problem can be partially overcome by making the prepulse potential (V_1 , eq. 1) longer and more positive, however, these measures do not guarantee that maximal P_o reaches unity in all conditions. Consequently, $V_{1/2}$ values obtained in those conditions can only be treated as 'apparent'.

Another problem may arise from the fact that some mutations and pharmacological agents shift voltage dependence of one or both gating processes to very positive potentials, so P_o of one or both gates is very low at potentials at which current components can be reliably separated. Consequently, data points calculated from eqs. 8 and 9 are not sufficient for the construction of the Boltzmann curve. In the case of voltage dependence of only one of the gating processes being shifted, the P_o curve obtained from the tail currents can be divided by the P_o curve obtained for one of the gates to yield the P_o curve of another gate that cannot be constructed using data points.

Despite numerous assumptions that need to be made for this method to work and, in extreme conditions, possible errors in determining parameters of the Boltzmann distribution, this method gives very clear qualitative measure of whether fast, slow, or both gates are affected by certain drugs and/or mutations.

Data to estimate CPP apparent binding affinity have been fitted with a one-site binding hyperbola of the form:

$$\Delta V_{1/2} = \Delta V_{1/2}^{\max} \frac{[\text{CPP}]}{(\text{EC}_{50} + [\text{CPP}])} \quad (11)$$

where $\Delta V_{1/2}$ represents the shift in $V_{1/2}$ produced by addition of CPP, $\Delta V_{1/2}^{\max}$ represents the maximal shift in $V_{1/2}$ produced by addition of CPP and EC_{50} is the concentration of CPP required to attain a half-maximal effect.

Results are presented as mean \pm S.E.M. Analysis for statistical significance used the paired t test or unpaired t test where appropriate (two-tailed).

Results

Kinetics of Inward Current Deactivation and Open Probability of Mutant hCIC-1.

One of the most characteristic features of the WT CIC-1 channel is that it deactivates with a double exponential time course to a new steady state when stepped to a membrane potential more negative than the Cl^- equilibrium potential (Fahlke et al., 1996; Rychkov et al., 1996; Accardi and Pusch, 2000). Mutations introduced to different places in the primary structure of the CIC-1 channel can drastically change the kinetics of current deactivation (Fahlke et al., 1997). Substitution of the phenylalanine residue at position 307 with a serine residue or substitution of the alanine at position 313 with a threonine residue resulted in a faster deactivation of the current at negative potentials than in WT CIC-1 (Fig. 1). The 100-ms prepulse to $+40$ mV was sufficient for maximal activation of WT channel (Fig. 1A), although both mutants required longer prepulses to more positive potentials. Therefore, a different voltage protocol has been used for mutant channels with a 200-ms prepulse to $+120$ mV followed by voltage steps ranging from -120 to $+120$ mV in 20 mV increments (Fig. 1, B and C).

Analysis of the current kinetics showed that the faster deactivation in both mutants was primarily caused by a significant decrease ($P < 0.05$; $n = 5$ to 7) of the time constant τ_2 of the slow exponential component (Fig. 2A). In addition, both mutations increased the relative amplitude of the second exponential component, a_2 , and decreased the steady state component, c , without a significant change in the relative amplitude of the fast exponential component, a_1 (Fig. 2, B–D).

Voltage dependence of the P_o of these mutants was shifted to more depolarized potentials (Fig. 3A). In the F307S mutant, the voltage of half-maximal P_o ($V_{1/2}$) was shifted by 74 mV from ~ -90 mV characteristic of WT hCIC-1 to ~ -16 mV; in the second mutant, A313T, the $V_{1/2}$ of channel activation was shifted even further toward more positive potentials by 113 mV when compared with WT, to a value of ~ 23 mV. As mentioned previously, CIC-1 has two types of gates, fast and slow. Consequently, P_o curves obtained from normalized tail currents, as presented in Fig. 3A, show the probability of both gates being open. It is possible, however, to derive separate P_o values for the fast and slow gating from the relative amplitudes of the exponential and the steady state components of the deactivating inward whole cell currents as described under *Materials and Methods*. Neither the F307S nor the A313T mutation shifted the fast gating but did significantly shift the P_o of the slow gating to the right along the voltage axes and drastically reduced the minimal P_o of the slow gate (Fig. 3, B and C; Table 1). As the P_o of the slow gate in the mutant channels was shifted to positive potentials by more than 70 mV, data points calculated from eq. 9 were insufficient for the reliable fit by Boltzmann distribution. Therefore, P_o curves for both mutants presented in Fig. 3C were obtained by dividing the P_o curve derived from peak tail currents (Fig. 3A) by the P_o curve of the fast gate (Fig. 3B) (see eq. 3). For the WT channel, the direct fit of the data points by the Boltzmann distribution and the above method of deriving P_o curve of the slow gate gave similar results with a typical difference between $V_{1/2}$ of less than 10 mV (Fig. 3C).

It is known that P_o of WT CIC-1 depends on the external Cl^- with the $V_{1/2}$ shifted by ~ 58 mV per decade of the Cl^-

TABLE 1

Effects of Cl^- concentration, mutations, and CPP on $V_{1/2}$ and minimal P_o of the fast and slow gates.

Both parameters are determined by fitting the Boltzmann distribution to open probabilities calculated from the relative amplitudes of the inward current components.

		Fast Gate	Fast Gate + CPP	Slow Gate	Slow Gate + CPP
WT, 178 mM Cl^-	$V_{1/2}$ (mV)	-120 ± 2	-63 ± 2	-78 ± 3	-64 ± 3
	P_{\min}	0.10 ± 0.02	0.15 ± 0.01	0.41 ± 0.03	0.45 ± 0.02
F307S, 178 mM Cl^-	$V_{1/2}$ (mV)	-106 ± 2	-52 ± 2	-15 ± 3	-8 ± 3
	P_{\min}	0.05 ± 0.02	0.07 ± 0.02	0.04 ± 0.02	0.04 ± 0.01
A313T, 178 mM Cl^-	$V_{1/2}$ (mV)	-111 ± 3	-56 ± 1	21 ± 1	37 ± 4
	P_{\min}	0.05 ± 0.02	0.06 ± 0.01	0.03 ± 0.01	0.06 ± 0.01
WT, 40 mM Cl^-	$V_{1/2}$ (mV)	-77 ± 3	-17 ± 1	-38 ± 3	-18 ± 4
	P_{\min}	0.09 ± 0.03	0.11 ± 0.01	0.35 ± 0.03	0.46 ± 0.02
F307S, 40 mM Cl^-	$V_{1/2}$ (mV)	-68 ± 3	-17 ± 1	35 ± 2	53 ± 4
	P_{\min}	0.05 ± 0.05	0.12 ± 0.01	0.05 ± 0.01	0.08 ± 0.01
A313T, 40 mM Cl^-	$V_{1/2}$ (mV)	-71 ± 3	-24 ± 5	77 ± 2	90 ± 3
	P_{\min}	0.14 ± 0.03	0.20 ± 0.03	0.04 ± 0.03	0.07 ± 0.02
WT, 8 mM Cl^-	$V_{1/2}$ (mV)	-56 ± 3		-12 ± 3	
	P_{\min}	0.04 ± 0.02		0.33 ± 0.02	

concentration change (Rychkov et al., 1996, 2001; Aromataris et al., 1999). Gating of both mutants was also sensitive to the external Cl^- , the dependence of $V_{1/2}$ on the \log of Cl^- concentration in both mutants was linear between 8 and 356 mM external Cl^- , with the slope of the line the same as that of the WT channel (Fig. 4A). The dependence of $V_{1/2}$ on Cl^- was shifted to higher Cl^- concentrations in both mutants. These results indicate that, compared with the WT channel, 15 and 85 times more Cl^- is required in the external solution for the F307S and A313T mutants, respectively, to open 50% of the channels at a particular voltage. When the P_o of the two types of gating of the WT channel were separated, it became apparent that reduction of the external Cl^- concentration shifted both fast and slow gating P_o to more positive potentials in parallel (Fig. 4B; Table 1). Similar parallel shift of the voltage dependence of both gating processes was also evident in the mutant channels (Table 1).

Effect of CPP on Fast and Slow Gating in WT and Mutant hCIC-1. To determine whether chemically induced myotonia has the same mechanism of action as the naturally occurring myotonia caused by the mutations, we compared the effects of CPP on the WT channel with the effects of the F307S and A313T mutations and investigated the effects of

CPP on these mutant channels. Application of 3 mM CPP to the bath solution produced faster inactivating currents from WT channels (Fig. 5A) that were superficially similar to the currents of the mutant channels in the control conditions; and also shifted P_o of the WT channel to more positive potentials by ~ 50 mV (not shown) as reported previously (Aromataris et al., 1999). Analysis of the relative amplitudes of the inward current components, however, revealed that CPP increased the amplitude of the fast exponential component and decreased the amplitude of the second exponential component (Fig. 5B) in clear contrast to the effects of the mutations on these inward current components (Fig. 2, B and C). The contrasting effects of CPP and mutations on the relative amplitudes of the current components indicate clearly that they have fundamentally different effects on the gating of CIC-1. In fact, application of 3 mM CPP to the WT channel shifted the fast gating toward positive potentials by ~ 60 mV, while shifting slow gating by only ~ 20 mV (Fig. 5C; Table 1).

In mutant channels, CPP produced changes in current kinetics similar to those seen in the WT channel (Fig. 6, A and B), but it was much less effective at shifting the $V_{1/2}$ of the mutant channels than the WT channel (Fig. 6C). The apparent K_d value of the CPP effect on the P_o of CIC-1 was 1.3

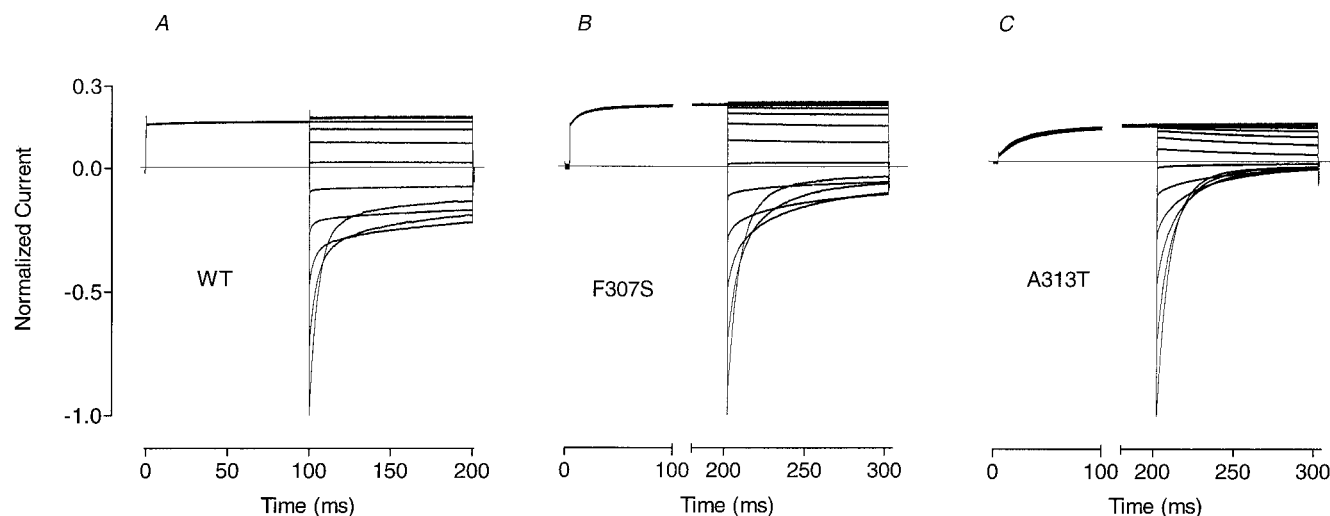


Fig. 1. Effect of mutations causing dominant myotonia congenita on CIC-1 currents. CIC-1 currents recorded from HEK293 cells expressing WT channel (A), F307S mutant (B), and A313T mutant (C). Voltage protocol: A, prepulse to $+40$ mV followed by the voltage steps ranging from -120 mV to $+80$ mV in 20 -mV increments; B and C, prepulse to $+120$ mV followed by the voltage steps ranging from -120 mV to $+120$ mV in 20 -mV increments. Holding potential -30 mV. Currents are normalized to the peak current amplitude at -120 mV.

mM for the WT channel, which increased to 4.6 mM and 7.5 mM for F307S and A313T, respectively. Separate effects of CPP on fast and slow gating of mutant channels, however, were very similar to that on fast and slow gating of the WT channel. Addition of 3 mM CPP shifted P_o of the fast gate of both mutant channels by ~ 50 mV, while shifting P_o of the slow gate by ~ 20 mV (Fig. 6, D and E; Table 1).

Discussion

The ClC-0 chloride channel from the *Torpedo californica* electric organ, which is 55% homologous to ClC-1, has been extensively studied on a single channel level and is known for its double-barrelled behavior and two independent gating processes, fast and slow (Hanke and Miller, 1983). Fast gating controls each pore independently on a millisecond time scale, whereas slow gating opens and closes both pores simultaneously on a much longer time scale. Recently, it became apparent from single-channel recording of ClC-1 that it also has two gating processes, similar to ClC-0 (Saviane et al., 1999). These findings showed that the time course of the inward current deactivation reflected the relaxations of the fast and slow gates of ClC-1. Because of its very low conductance, ClC-1 is not easily amenable to single channel recording, and most experiments are restricted to the macroscopic

currents. To separate P_o of the fast and slow gating from the macroscopic currents, Accardi and Pusch (2000) used envelope protocols. These envelope protocols could only be used on membrane patches with small capacitance, because they required very short (~ 200 μ s) prepulses to positive potentials. In the present work, we used a different method of separation of the P_o of the fast and slow gating from the whole cell currents. This method and the one based on the envelope protocols give very similar qualitative results (compare Accardi and Pusch, 2000). The biggest difference obtained by these two methods is in the minimal P_o of both gates of the WT channel, which were significantly larger in the study by Accardi and Pusch (2000). The reasons for this could be the different modes employed for recording macroscopic currents: the earlier study used inside-out patches whereas we used the whole cell; in addition, there was a difference in cytoplasmic Cl^- concentration: 100 mM versus 40 mM. In ClC-0, expressed in *Xenopus laevis* oocytes, the minimal P_o of the fast gate was significantly lower in the two-electrode voltage clamp than in cell-attached patches and it was also reduced with a lower cytoplasmic Cl^- concentration (Ludewig et al., 1997).

A dominant mode of inheritance of the mutations causing Thomsen's disease is explained by a dominant negative effect

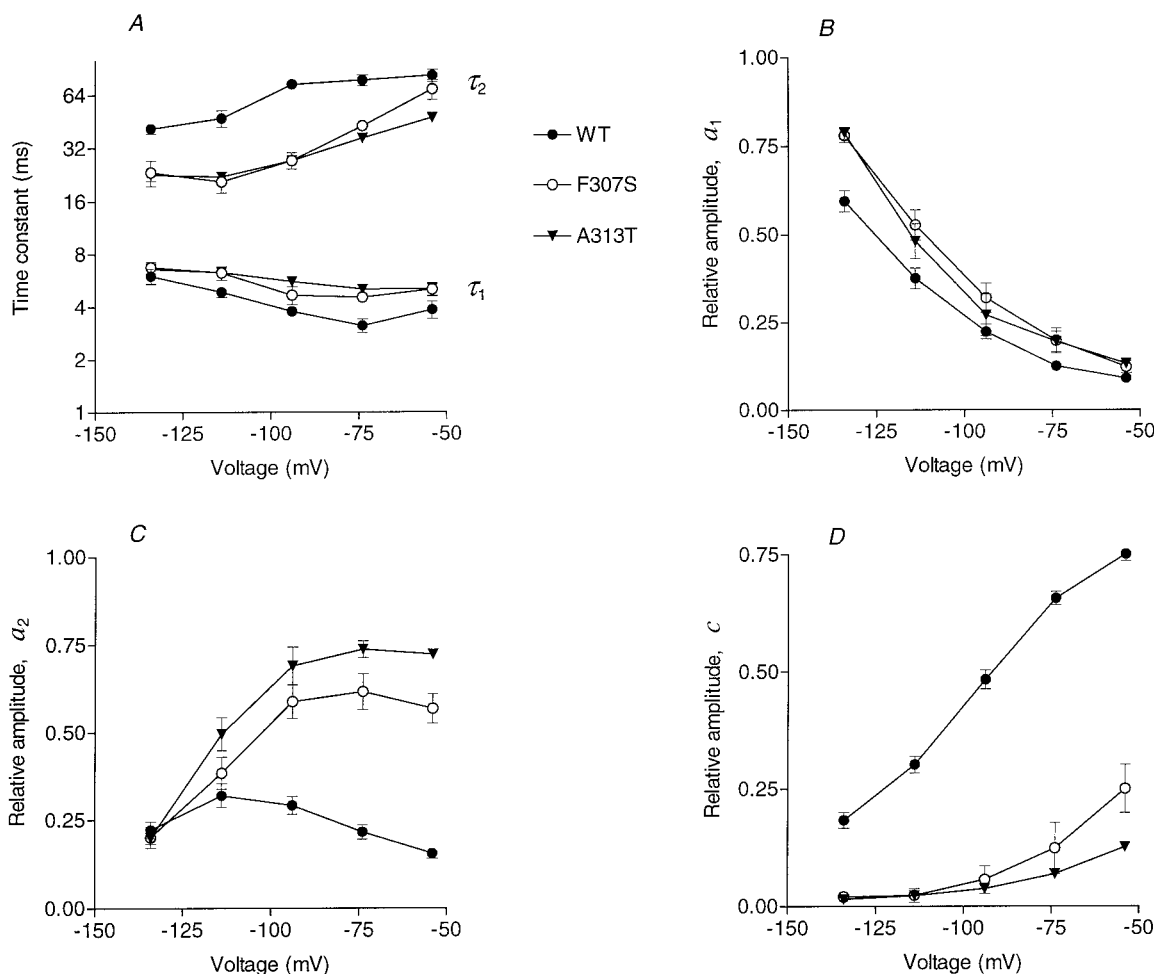


Fig. 2. Effect of myotonic mutations on kinetics of inward current deactivation. A, time constants of the fast (τ_1) and slow (τ_2) exponential components of the inward current. Relative amplitudes of the inward current components of the WT and mutant channels: fast exponential component a_1 (B); slow exponential component a_2 (C); and time-independent component c (D; see eq. 7).

of the mutated subunit on the WT subunit in a multimeric complex (Pusch et al., 1995b; Kubisch et al., 1998). It has been shown that the $V_{1/2}$ of the heteromeric mutant/WT complexes is often shifted drastically to more positive potentials (Pusch et al., 1995b) and that the mechanism of this shift lies in the slow gate common to both pores of the ClC-1 channel dimer (Saviane et al., 1999). The results of the present work support this hypothesis; in both mutant channels, F307S and A313T, slow gating was shifted to more positive potentials. Moreover, unlike another dominant mutant, I290M, in which both fast and slow gating were shifted simultaneously (Saviane et al., 1999), mutations F307S and A313T shifted P_o of only the slow gating without much effect on the fast gating mechanism (Fig. 6, D and E). Comparison of the effects of CPP and these dominant myotonic mutations

on ClC-1 gating revealed that although they cause similar changes in voltage dependence of ClC-1 P_o , they do not share the same mechanism of action. Unlike F307S and A313T mutations, CPP mainly shifts voltage dependence of the fast gating. These results once more support the notion that the fast and slow gates of ClC channels are different structures and can be manipulated separately. CPP represents an interesting example in this respect. Open probabilities of the F307S and A313T mutants obtained from the normalized tail currents were plainly much less sensitive to CPP than WT. CPP in 3 mM concentration shifted P_o curves in WT by ~ 50 mV, whereas in F307S, the shift was ~ 25 mV and in A313T only ~ 12 mV (Fig. 6C). When P_o of fast and slow gating were separated, it turned out that 3 mM CPP affected fast gating of the mutant channels to the same extent as the fast gating

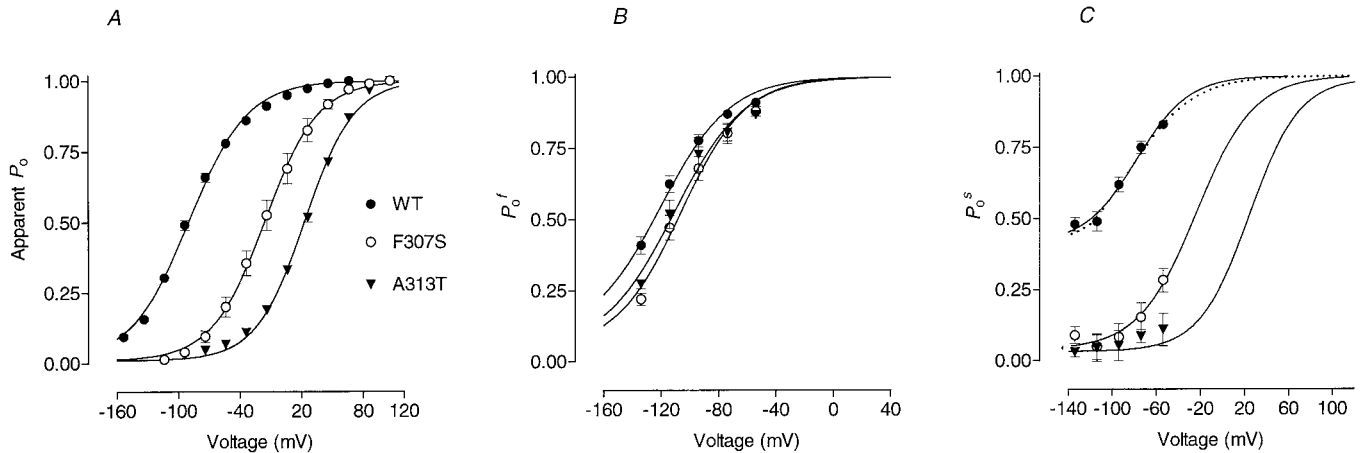


Fig. 3. Effect of myotonic mutations on ClC-1 P_o . A, apparent P_o curves for WT and mutant channels. Apparent P_o was estimated from the peak tail currents after the voltage steps to different membrane potentials (Rychkov et al., 1996; Aromataris et al., 1999). Solid lines represent the Boltzmann distribution (eq. 10). B and C, open probability of the fast and the slow gates, respectively. Data points were calculated from the relative amplitudes of the components of the inward currents as explained under *Materials and Methods*. In B, solid lines represent the Boltzmann distribution fitted to the calculated data points. In C, solid lines were obtained by dividing the P_o curves derived from peak tail currents shown in A by the P_o curve of the fast gate shown in B (see eq. 3). For the slow gating of both mutants, data was insufficient for a reliable fit by the Boltzmann distribution. Dotted line represents the Boltzmann distribution fitted to the data points calculated for the WT channel.

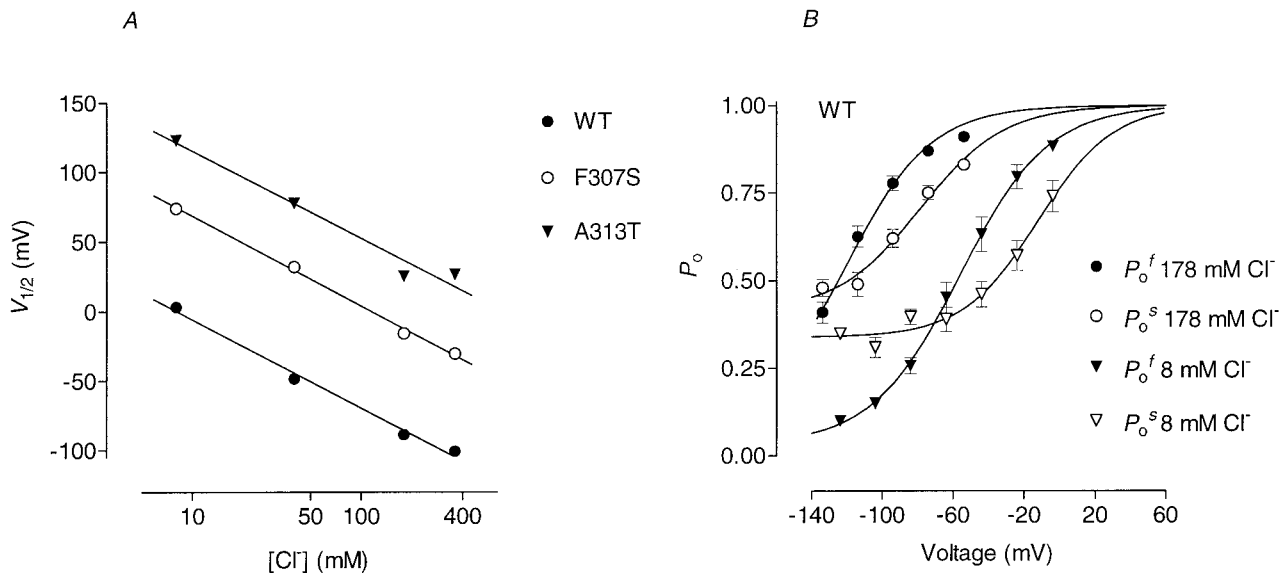


Fig. 4. Dependence of P_o of the WT and mutant channels on the external Cl^- concentration. A, voltage of the half-maximal P_o ($V_{1/2}$) of WT and mutant channels, obtained from tail currents is plotted against the \log of the external Cl^- concentration change. B, P_o curves of the fast and slow gating of the WT ClC-1 in different external Cl^- concentrations. Solid lines represent the Boltzmann distributions fitted to the calculated data points (eqs. 8 and 9).

of WT. Therefore, the apparent change of affinity of CPP in the mutant channels could not be caused by a change of the CPP binding to its site. In the mutant channels, the voltage dependence of P_o of different gates are separated to a such an extent that when the slow gate just starts to open, P_o of the fast gate is already close to its maximal value. Consequently, slow gating is the main contributor to the channel's overall P_o obtained from the normalized tail currents, so only the effect of CPP on the slow gate is evident, whereas its effect on the fast gate remains hidden.

A shift in the voltage dependence of channel P_o implies that voltage-dependent steps in channel transition from closed to open states have somehow been altered. A detailed model of CIC-1 gating that would explain all known properties of the channel is yet to be developed, but three models of gating of either CIC-0 or CIC-1 have been proposed. The model for CIC-1 that includes an intrinsic voltage sensor (Fahlke et al., 1996) in the protein structure of the channel is not supported by some of the experimental data, as has been described previously (Saviane et al., 1999; Accardi and Pusch, 2000) and will not be discussed

here. Both of the other models proposed to explain voltage and Cl^- dependence of fast gating of CIC-0 are based on the assumption that the permeating anion also provides the gating charge. Pusch et al. (1995a) suggested that the pore of the channel contains two binding sites for Cl^- and the fast gate is situated closer to the cytoplasmic side of the channel than the inner site. Occupation of this inner site by Cl^- shifts the equilibrium between open and closed states to the open state. Voltage dependence of the gating in this model was attributed to the Cl^- movement from the outer to the inner site. According to this model, alteration of the inner site affinity for Cl^- or a change in the energy barrier for Cl^- between two sites could lead to a shift of the P_o along the voltage axes. Change in the inner site affinity for Cl^- was proposed to be a reason for the shift of CIC-1 P_o in the presence of CPP (Aromataris et al., 1999). However, the recent finding that the time constant of fast gating does not saturate at very high positive potentials, at which Cl^- binding to the inner site should be saturated (Accardi and Pusch, 2000), is more consistent with a model of the kind proposed by Chen and Miller (1996). The latter model

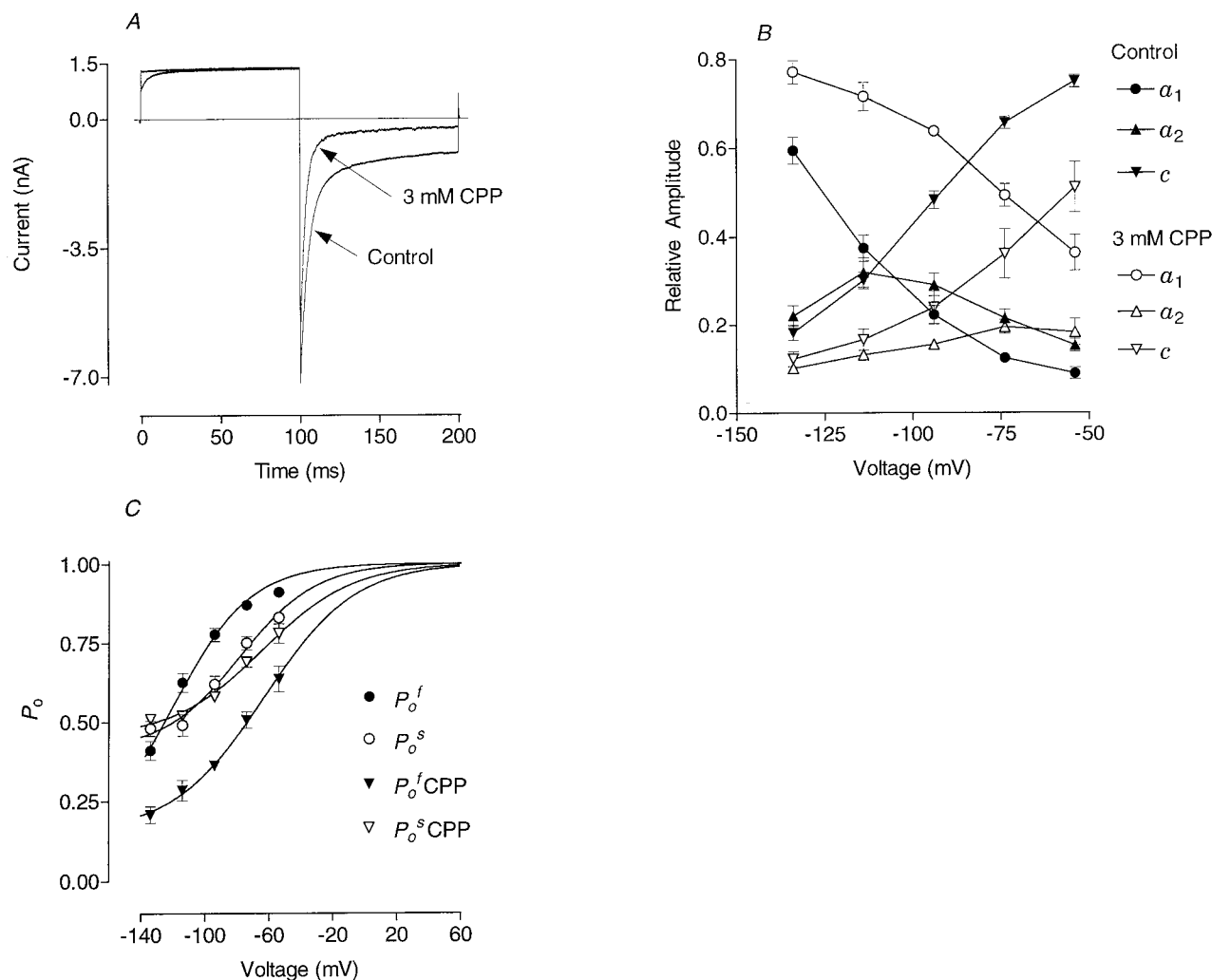


Fig. 5. Effect of the external application of CPP on the currents and P_o of the WT channel. A, wild-type CIC-1 currents recorded in response to a voltage step to -120 mV after a prepulse to $+40$ mV in control conditions and in the presence of 3 mM CPP in the external solution. Holding potential -30 mV. B, relative amplitudes of the inward current components of the WT CIC-1 inward currents in the control conditions and the presence of 3 mM CPP. C, P_o curves of the fast and slow gating of the WT channel in control conditions and in the presence of 3 mM CPP. Solid lines represent the Boltzmann distributions fitted to the calculated data points (eqs. 8 and 9).

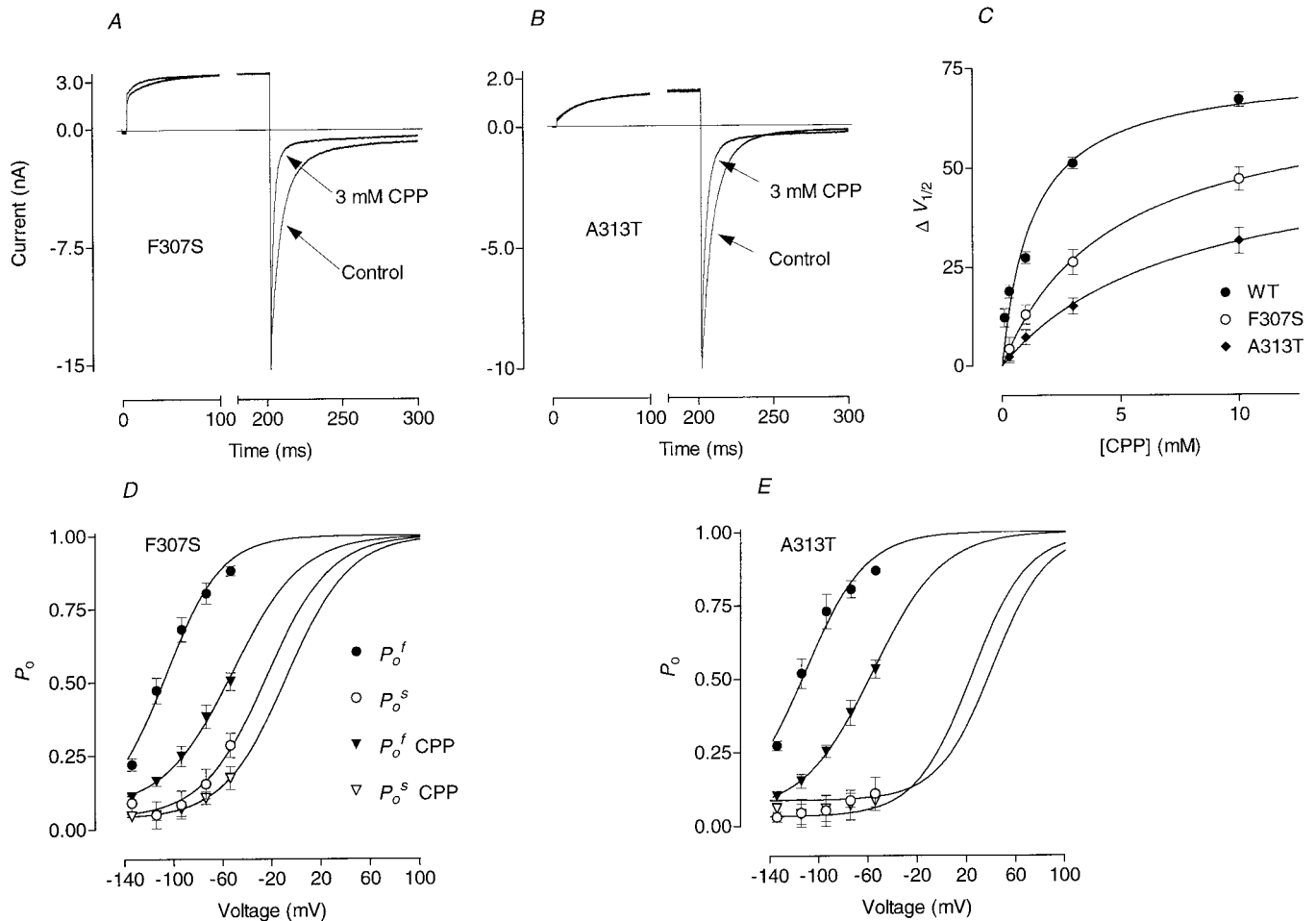


Fig. 6. Effect of the external application of CPP on the currents and P_o of the mutant channels. A and B, mutant ClC-1 currents recorded in response to a voltage step to -120 mV after a prepulse to +120 mV in control conditions and in the presence of 3 mM CPP in the external solution. Holding potential -30 mV. C, shift of the $V_{1/2}$ ($\Delta V_{1/2}$) of the WT and mutant channels in the presence of different concentrations of CPP in the external solution. Experimental data points are fitted with a one-site binding hyperbola (eq. 11). D and E, fast and slow gate P_o of the mutant channels in the control conditions and in the presence of 3 mM CPP in the external solution. For the fast gate, the Boltzmann distributions were fitted to the calculated data points; for the slow gate, curves were obtained as in Fig. 3C.

suggested that the binding site for Cl^- is located externally, and the voltage dependence of channel gating arises from transfer of the bound Cl^- across the electric field during the conformational change of the channel protein, with the channel opening rate strongly dependent on both voltage and Cl^- concentration.

Results of the present work taken together with the previous studies could provide some clue about what exactly is changed in mutant channels or in the presence of CPP: the affinity of the gating site for Cl^- or the free energy of transition between closed and open states. Open probabilities of both gates shift in parallel with changing Cl^- concentration (Fig. 4B), which suggests that both gates depend on Cl^- binding to the same site. In this case, alteration of Cl^- binding to that site will lead to the shift of both fast and slow gating. CPP predominantly shifted fast gating in the WT channel, and the mutations F307S and A313T affected the slow gate, so it is unlikely that the mechanism of their action would be on the Cl^- binding site; rather, it would be on the voltage dependent transformation to an open state that follows after Cl^- binding.

Acknowledgments

We are grateful to Professor T. J. Jentsch of the Center for Molecular Neurobiology (Hamburg, Germany) for providing the human ClC-1 clone. We dedicate this work to the memory of Shirley Bryant, who made fundamental contributions toward elucidating the involvement of chloride channels in myotonia. He passed away on July 21, 1999.

References

- Accardi A and Pusch M (2000) Fast and slow relaxations in the muscle chloride channel ClC-1. *J Gen Physiol* **116**:433–444.
- Aromataris EC, Astill DS, Rychkov GY, Bryant SH, Bretag AH and Roberts ML (1999) Modulation of the gating of ClC-1 by S-(+)-2-(4-chlorophenoxy) propionic acid. *Br J Pharmacol* **126**:1375–1382.
- Barry PH (1994) JPCalc, a software package for calculating liquid junction potential corrections in patch-clamp, intracellular, epithelial and bilayer measurements and for correcting junction potential measurements. *J Neurosci Methods* **51**:107–116.
- Bryant SH and Morales-Aguilera A (1971) Chloride conductance in normal and myotonic muscle fibres and the action of monocarboxylic aromatic acids. *J Physiol* **219**:367–383.
- Chen TY and Miller C (1996) Nonequilibrium gating and voltage dependence of the ClC-0 Cl^- channel. *J Gen Physiol* **108**:237–250.
- Conte Camerino D, Tortorella V, Bettoni G, Bryant SH, De Luca A, Mambrini M, Tricarico D and Grasso G (1988) A stereospecific binding site regulates the Cl^- ion channel in rat skeletal muscle. *Pharmacol Res Commun* **20**:1077–1078.
- Dromgoole S, Campion D and Peter J (1975) Myotonia induced by clofibrate and sodium chlorophenoxy isobutyrate. *Biochem Med* **14**:238–240.

- Fahlke C, Rosenbohm A, Mitrovic N, George AL and Rüdel R (1996) Mechanism of voltage-dependent gating in skeletal muscle chloride channels. *Biophys J* **71**:695–706.
- Fahlke C, Yu HT, Beck CL, Rhodes TH, and George AL (1997) Pore-forming segments in voltage-gated chloride channels. *Nature (Lond)* **390**:529–532.
- Hanke W and Miller C (1983) Single chloride channels from *Torpedo* electroplax. *J Gen Physiol* **82**:25–45.
- Ho SN, Hunt HD, Horton RM, Pullen JK and Pease LR (1989) Site-directed mutagenesis by overlap extension using the polymerase chain reaction. *Gene* **77**:51–59.
- Jentsch TJ, Friedrich T, Schriever A and Yamada H (1999) The ClC chloride channel family. *Pfluegers Arch* **437**:783–795.
- Koch MC, Steinmeyer K, Lorenz C, Ricker K, Wolf F, Otto M, Zoll B, Lehmann-Horn F, Grzeschik KH and Jentsch TJ (1992) The skeletal muscle chloride channel in dominant and recessive human myotonia. *Science (Wash DC)* **257**:797–800.
- Kubisch C, Schmidt-Rose T, Fontaine B, Bretag AH, and Jentsch TJ (1998) ClC-1 chloride channel mutations in myotonia congenita: variable penetrance of mutations shifting the voltage dependence. *Hum Mol Genet* **7**:1753–1760.
- Langer T and Levy R (1968) Acute muscular syndrome associated with administration of clofibrate. *N Engl J Med* **279**:856–858.
- Lorenz C, Pusch M and Jentsch TJ (1996) Heteromultimeric ClC chloride channels with novel properties. *Proc Natl Acad Sci USA* **93**:13362–13366.
- Lloyd S, Pearce SHS, Fisher SE, Steinmeyer K, Schwappach B, Seeman SS, Harding B, Bolino M, Devoto M, Goodyer P, et al. (1996) A common molecular basis for three inherited kidney stone diseases. *Nature (Lond)* **379**:445–449.
- Ludewig U, Jentsch TJ and Pusch M (1997) Analysis of a protein region involved in permeation and gating of the voltage-gated *Torpedo* chloride channel ClC-0. *J Physiol* **498**:691–702.
- Pusch M, Liantonio A, Bertorello L, Accardi A, De Luca A, Pierro S, Tortorella V, and Conte Camerino D (2000) Pharmacological characterization of chloride channels belonging to the ClC family by the use of chiral clofibric acid derivatives. *Mol Pharmacol* **58**:498–507.
- Pusch M, Ludewig U, Rehfeldt A, and Jentsch TJ (1995a) Gating of the voltage-dependent chloride channel ClC-0 by the permeant anion. *Nature (Lond)* **373**:527–531.
- Pusch M, Steinmeyer K, Koch MC and Jentsch TC. (1995b) Mutations in dominant human myotonia congenita drastically alter the voltage-dependence of the ClC-1 chloride channel. *Neuron* **15**:1455–1463.
- Rychkov GY, Pusch M, Astill DS, Roberts ML, Jentsch TJ and Bretag AH (1996) Concentration and pH dependence of skeletal muscle chloride channel ClC-1. *J Physiol* **497**:423–435.
- Rychkov GY, Pusch M, Roberts ML and Bretag AH (2001) Interaction of hydrophobic anions with skeletal muscle chloride channel ClC-1: effects on permeation and gating. *J Physiol* **530**:379–393.
- Saviane C, Conti F and Pusch M (1999) The muscular chloride channel ClC-1 has a double barrelled appearance that is differentially affected in dominant and recessive myotonia. *J Gen Physiol* **113**:457–468.
- Simon DB, Bindra RS, Mansfield TA, Nelson-Williams C, Mendonca E, Stone R, Schurman S, Nayir A, Alpay H, Bakkaloglu A, et al. (1997) Mutations in the chloride channel gene. *CLCNKB*, cause Bartter's syndrome type III. *Nat Genet* **17**:171–178.
- Steinmeyer K, Lorenz C, Pusch M, Koch MC and Jentsch TJ (1994) Multimeric structure of ClC-1 chloride channel revealed by mutations in dominant myotonia congenita (Thomsen). *EMBO J* **13**:737–743.
- Wollnik B, Kubisch C, Steinmeyer K and Pusch M (1997) Identification of functionally important regions of the muscular chloride channel ClC-1 by analysis of recessive and dominant myotonic mutations. *Hum Mol Genet* **6**:805–811.

Address correspondence to: Dr. Grigori Rychkov, Center for Advanced Biomedical Studies, University of South Australia, North Terrace, Adelaide, SA 5000, Australia. E-mail: grigori.rychkov@adelaide.edu.au
